I R A M P
9(1), June 2018, pp. 7-12

ISSN: 2229-3159

Measurements of Laser Plasma Hypersonic Expansion Dynamics

GHANESHWAR GAUTAM[1] AND CHRISTIAN G. PARIGGER[2,*]

[1]Fort Peck Community College, 605 Indian Avenue, Poplar, MT 59255, USA
[2] University of Tennessee, University of Tennessee Space Institute, Center for Laser Applications, 411 B.H. Goethert Parkway, Tullahoma, TN 37388-9700, USA
**Corresponding author E-mail: cparigge@tennessee.edu (C.G. Parigger)*

ABSTRACT: Subsequent to generation of optical breakdown in gases with peak-power radiation in excess of 100 GW/cm^2, laser plasma expansions reveal speeds well in excess of supersonic, hypersonic, and re-entry speeds with Mach numbers of Ma > 1, Ma > 5, Ma > 25, respectively. The reported experiments utilize a Czerny-Turner type spectrometer and an intensified charge-coupled device; the former effectively acts as a narrow-band filter and the latter allows one to freeze images of the plasma expansion at high equivalent shutter speed. A 14-ns pulse-width, Nd:YAG laser device operated at the fundamental 1064-nm wavelength generates optical breakdown in ultra-high-pure hydrogen gas filled inside a cell at near ambient temperature and pressure, hydrogen gas at pressure of $(1.08 \pm 0.033) \times 10^5$ Pa. The hydrogen Balmer alpha line, H_α, displays significantly Stark-broadened and Stark-shifted profiles. Measurements of the vertical diameters of the spectrally resolved plasma images for time delays of 10 ns to 35 ns indicate expansion speeds that are of the order of 100 km/s to 10 km/s. For time delays in the range of 0.5 μs to 1 μs, the expansion speed decreases to 1.3 km/s, the speed-of-sound in hydrogen gas.

Keywords: Plasma diagnostics, atomic spectra, hypersonic flow, plasma spectroscopy, laser-induced breakdown spectroscopy.

PACS Codes: 52.70.-m, 32.30-r, 52.25.Jm, 42.62.Fi

1. INTRODUCTION

This work presents recorded expansion dynamics following laser plasma generation in hydrogen gas at a pressure slightly above 10^5 Pa. Study of the plasma expansion is of interest in astrophysical, engineering, scientific research as well as for various applications [1 - 5]. Astrophysical interests include interpretation of white dwarf photosphere absorption spectra by simulating conditions of these selected stars in laboratory settings [2 - 4] and by exploring laser-induced plasma [4] with time-resolved laser spectroscopy. The engineering and scientific research motivation [5] extends to the measurement of phenomena that occur at hypersonic to re-entry speeds that are in the Mach number range of Ma = 5 to Ma = 25, or above.

During the plasma expansion, spatial and temporal variations of density, temperature, and pressure are observed. Investigations of these spatial and temporal profiles allow us to infer the expansion speeds. Plasma at elevated temperature and pressure expands with high velocity and drives a shock wave into the outward direction. As the incident laser beam is focused to above breakdown threshold irradiance, breakdown occurs at a location before the pulse reaches its focal point [6]. The interaction between the laser beam and material is a complex process, and depends on many characteristics such as laser parameters or target material. Various factors affect the interaction including the properties such as the pulse width, spatial and temporal fluctuation of the pulse as well as the peak irradiance variations. For example, effects of pulse width on nascent laser-induced bubbles for underwater laser-induced breakdown spectroscopy (LIBS) show that a long pulse causes well-defined, clear line spectra. In turn, a short pulse usually causes considerably asymmetric or deformed spectra. However, this effect is more significant for

solid target material than for gases [7]. Moreover, images of laser-induced breakdown plasma in air [8] nicely illustrate expansion dynamics. Experimental results in air [8] show two distinct regions with higher intensity towards the laser propagation direction for time delays of 25 ns to 10 μs. Equally, Schlieren images of laser-induced plasma generated in air at standard ambient temperature and pressure show plasma jet propagation towards the laser for time delays of 1 μs to 20 μs [9]. However, the jet propagation direction depends on the type of gas, the gas pressure, the ratio of energy absorbed in the plasma and the threshold irradiance for occurrence of optical breakdown [9].

2. EXPERIMENTAL DETAILS

Figure 1 illustrates the experimental schematic. For the experiments, ultra-high-pure hydrogen gas is filled inside a cell at pressure of $(1.08 \pm 0.033) \times 10^5$ Pa.

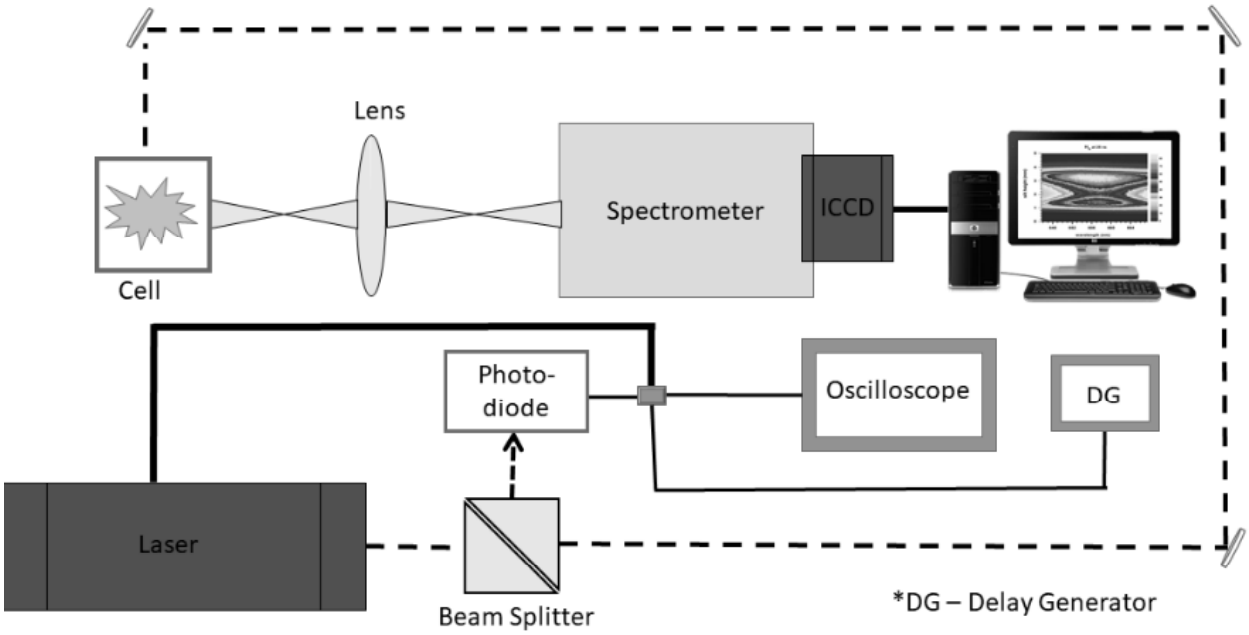

Figure 1. Experimental schematic for time-resolved laser spectroscopy

In the study of time-resolved and space-resolved plasma emission spectroscopy, a Q-switched Nd:YAG laser device is operated at its fundamental wavelength of 1064 nm with 10 Hz repetition rate and 14 ns full-width-half-maximum pulses. The measured energy per pulse is 120 mJ. The laser beam was passed through a dichroic beam splitter to remove the residual 532 nm component. A silicon photodiode detector was used to record a portion of the laser radiation reflected off of the beam splitter at the exit of the laser source. The photodiode is connected to the oscilloscope to monitor the optical pulse. Three Thorlab mirrors align the beam parallel to the spectrometer slit.

A holographic grating of 1200 grooves/mm is selected to disperse the radiation from the plasma. For the recording of temporally and spatially resolved plasma emission spectra images along the slit height, the following instrumentation is employed: Czerny-Turner type spectrometer (0.64 m - HR640; Jobin-Yvon) and 2-dimensional integrated charged coupled device (ICCD). The spectral resolution amounted to 0.11 nm. The data were recorded with a 5 ns gate width and an average of 100 consecutive laser-plasma events were accumulated. For later time delays of 400 ns and 900 ns, 20 ns gate width and 50 consecutive laser-plasma events were accumulated. The recorded spectra are wavelength calibrated and corrected for detector sensitivity. Matlab® scripts are utilized for wavelength calibration and sensitivity correction, and Origin Software is employed for graphical display of the experimental data.

In laser-induced plasma, the ambient gas usually affects the plasma expansion. Pressure and types of gases also influence post-breakdown phenomena. For example, at low pressure, the losses and uniformity of the plasma energy

distribution increase [1]. Plasma size, propagation speed, and emission property are also related to the ambient gas into which the plasma expands. The physical cause of high-speed expansion is the large pressure difference between the plasma and its surrounding environment. However, this work investigates expansion dynamics in near standard ambient temperature and pressure (SATP) hydrogen gas.

3. RESULTS

This section elaborates on the determination of the expansion speed of the micro-plasma generated in the ultra-high-pure hydrogen gas inside a cell. Experimental results shows high plasma expansion speeds of 100 km/s to 10 km/s at early time delays of 10 ns to 35 ns.

Figure 2 display the recorded H_α plasma spectra at early time delays of 10 ns to 35 ns, in 5-ns steps. The two-dimensional spectra of slit-height versus wavelength are significantly Stark-broadened and Stark-shifted at early time delays. The measured intensity is increasing for successive time delays. However, the area and line-width of the spectral profiles decrease continuously, implying decreasing electron density. From the recorded H_α plasma spectra at early time delay as displayed in Figure 2, plasma expansion speeds are determined. The diameter of the plasma in the lateral or slit-height direction is measured as a function of time, and hence the plasma expansion-speed can be determined. For example, the arrows on the spectra images at 10 ns and 15 ns in Figure 2 indicate the spatial plasma ranges used for the determination of the expansion speeds.

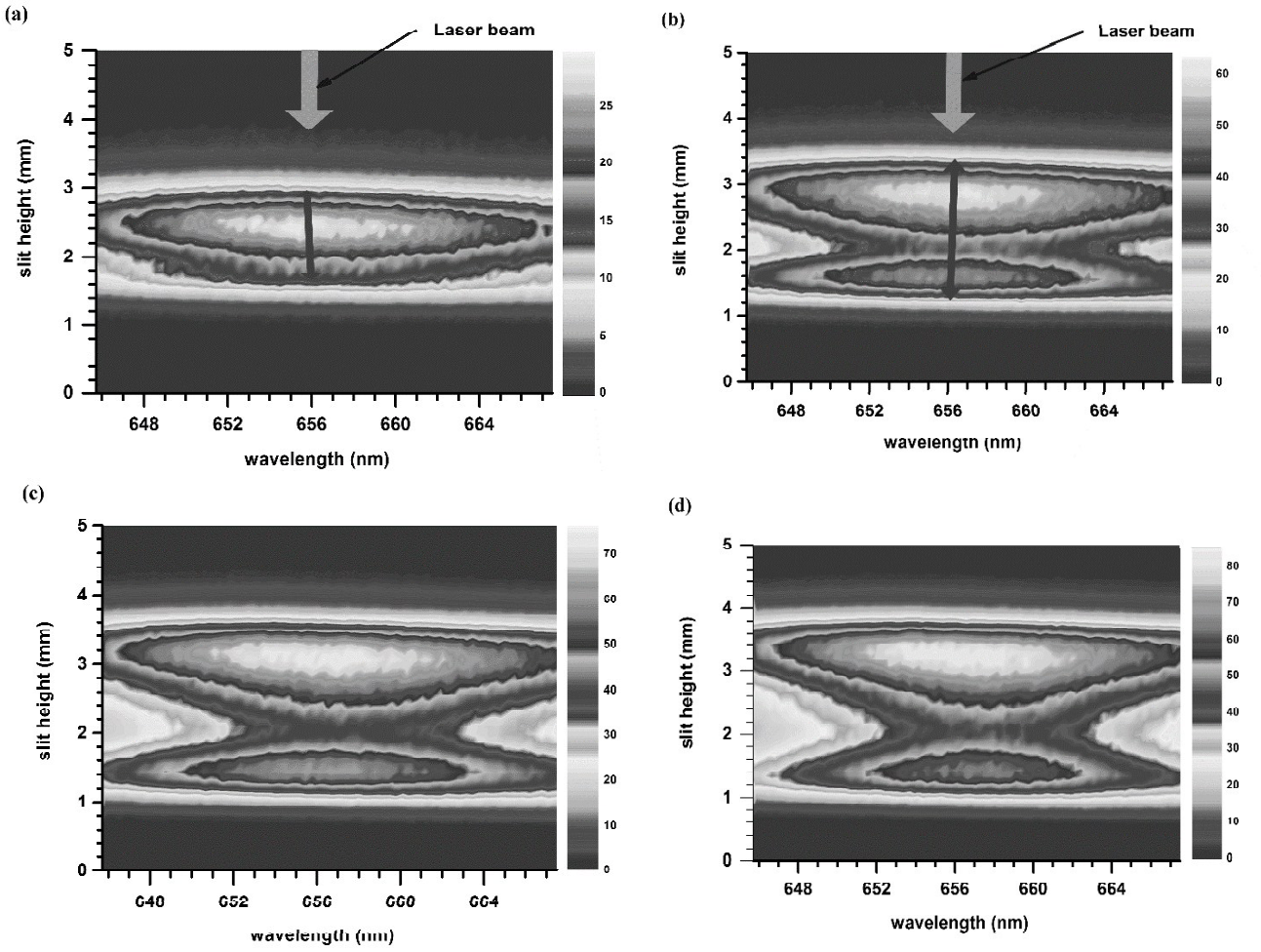

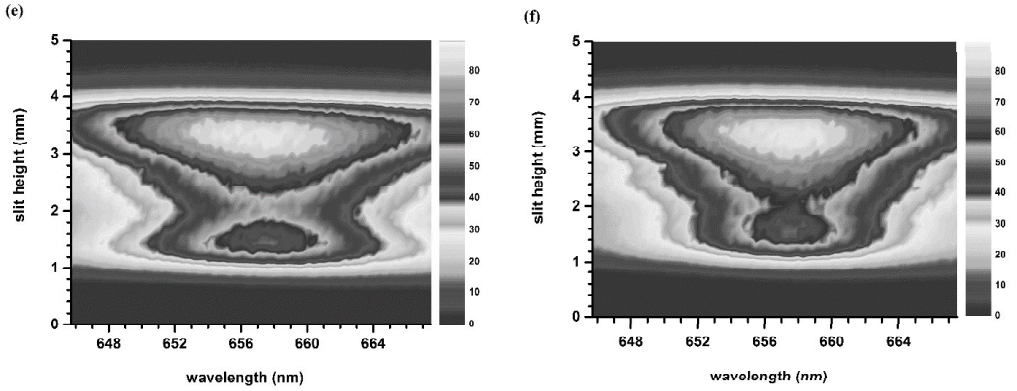

Figure 2. **Hydrogen alpha plasma spectra images for selected time delays:** (a) **10 ns;** (b) **15 ns;** (c) **20 ns;** (d) **25 ns;** (e) **30 ns; and** (f) **35 ns**

The recorded images of the laser-induced plasma with 14 ns pulses depict higher intensity towards the laser at early time delay of 10 ns to 35 ns. However, opposite behavior is observed at later time delay, e.g., for time delays of 400 ns. Figure 3 illustrates the experimental records for time delays of 400 and 900 ns.

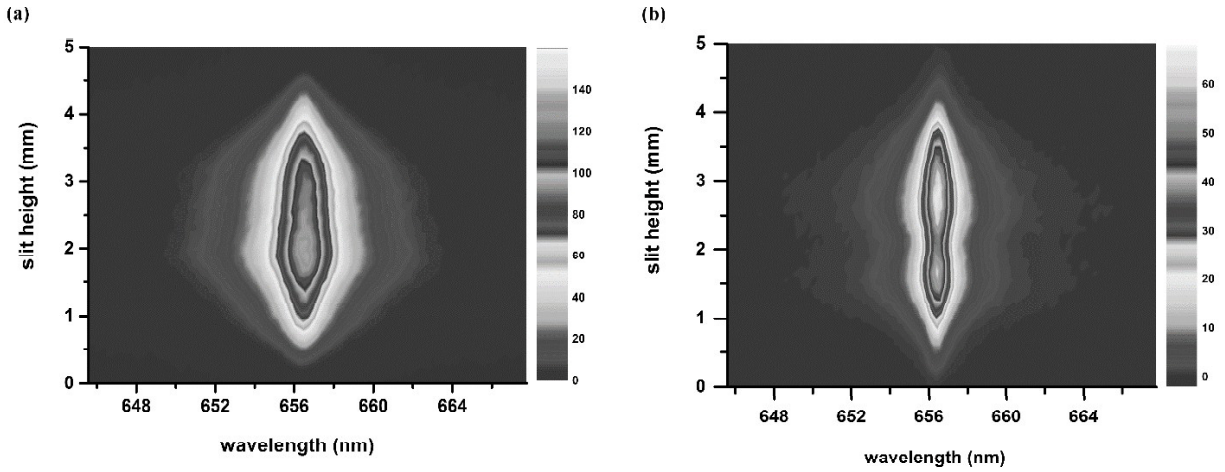

Figure 3. Hydrogen alpha plasma spectra images at time delays of (a) **400 ns and** (b) **900 ns.**

From the images in Figures 2 and 3, the diameter of the plasma in lateral or slit-height direction is measured as a function of time, and hence plasma expansion speeds can be diagnosed. Table 1 displays the measured diameters of the plasma and corresponding speeds at various time delays.

Table 1. Plasma Expansion Speed at Various Time Delays Obtained from Lateral Expansion in the Contour Plots of Figures 2 and 3

Time delay(ns)	Diameter(mm)	Distance in 5 ns(mm)	Expansion speed(km/s)
10	1.32	—	—
15	2.03	0.71	142
20	2.42	0.39	78
25	2.71	0.29	58
30	2.86	0.15	30
35	2.92	0.06	12
400	0.96	—	—
900	1.81	0.85*	1.70

*Distance for 500 ns.

The predicted plasma expansion speeds are of the order of 100 to 10 km/s for time delays in the range of 15 to 35 ns. The determined expansion speeds are well-above hypersonic speed (Mach number 5) or above re-entry speeds (Mach number 25) at these time delays. Figure 4 illustrates the tabulated results.

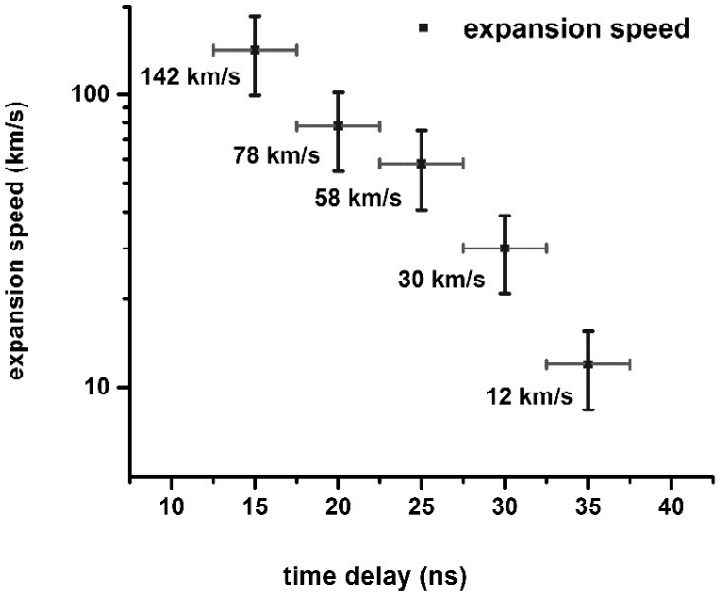

Figure 4. Plasma expansion speeds in semilog plot (see Table 1). The indicated time-delay error bars are due to the gate width of 5 ns

The plasma expansion decreases to typically hypersonic and sonic speeds for larger time delays as indicated in Figure 3 and Table 1. The measured expansion speeds are consistent with results communicated in previous experimental studies [10, 11]. However, computer simulations show a shock-wave expansion speed of 60 km/s at a time delay of 20 ns in air at atmospheric pressure [12], thereby indicating that the determined speeds are consistent with other experimental results. Note that the speed of sound in hydrogen gas is 1.3 km/s, or a factor of 3.5 higher than in ambient pressure and temperature air.

For longer time delays of about 1 μs, the images in Figure 3 are utilized for the diagnostics of the plasma expansion speed. The determined speed is 1.7 ± 0.5 km/s at 900 ns. The estimated error bars for these speeds are ± 30%. These result agree as well with those of recently communicated hydrogen experiments [13].

4. CONCLUSIONS

The laser-induced plasma expands with well-above hypersonic speed depending upon the ambient conditions and time delays. The spectra recorded during the evolution of the plasma are significantly Stark-broadened and Stark-shifted, therefore, a larger percentage error occurs for the predicted speeds for earlier time delays. For longer time delays, plasma expansion speeds decrease considerably, therefore, larger differences occur for the speed measurement due to the increased temporal interval. To improve the graphically inferred expansion speeds, Abel inversion methods can be applied so that radial information can be extracted from the recorded line-of-sight measurements [14]. The predicted expansion speeds may be useful for the NASA hypersonic technology (HT) project.

References

[1] F. Anabitarte, A. Cobo, J.M. Lopez-Higuera, *Int. Scholarly Res. Notes: Spectroscopy* **2012** (2012), 285240.

[2] R.E. Falcon, G.A. Rochau, J.E. Bailey, J.L. Ellis, A.L. Carlson, T.A. Gomez, M.H. Montgomery, D.E. Winget, E.Y. Chen, M.R. Gomez, T.J. Nash, *High Energy Density Physics* **9** (2013), 82.

[3] R.E. Falcon, G.A. Rochau, J.E. Bailey, T.A. Gomez, M.H. Montgomery, D.E. Winget, T. Nagayama, *Astrophy. J.* **806** (2015), 214.

[4] C.G. Parigger, K.A. Drake, C.M. Helstern, G. Gautam, G., *Atoms* **6** (2018), 33.

[5] R. Engeln, S. Mazouffre, P. Vankan, I. Bakker, D.C. Schram, Plasma Sources Science Technology **11** (2002), A100.

[6] Y.L. Chen, J.W.L. Lewis, C.G. Parigger, *J. Quant. Spectrosc. Radiat. Transfer* **67** (2000), 91.

[7] T. Sakka, A. Tamura, A. Matsumoto, K. Fukami, N. Nishi, B. Thornton, *Spectrochim. Acta Part B: At. Spectrosc.* **97** (2014), 94.

[8] N. Glumac, G. Elliott, M. Boguszko, *AIAA Journal* **34** (2005), 1984.

[9] S. Brieschenk, S. O'Byrne, H. Kleine, *Opt. Lett.* **38** (2013), 664.

[10] C.G. Parigger, D.H. Plemmons, J.W.L. Lewis, *Appl. Opt.* **34** (1995), 3325.

[11] C.G. Parigger, *Spectrochim. Acta Part B: At. Spectrosc.* **79** (2013), 4.

[12] H. Sobral, M. Villagrán-Muniz, R. Navarro-González, A.C. Raga, *Appl. Phys. Lett.* **77** (2000), 3158.

[13] C.G. Parigger, D.M. Surmick, G. Gautam, *J. Phys.: Conf. Ser.* **810** (2017), 012012.

[14] C.G. Parigger, G. Gautam, D.M. Surmick, *Int. Rev. At. Mol. Phys.* **6** (2015), 43.